Dynamics of Vicsek fractals, models for hyperbranched polymers

A. Blumen,[1] A. Jurjiu,[1] Th. Koslowski,[2] and Ch. von Ferber[1]
[1]*Theoretische Polymerphysik, Universität Freiburg, Hermann-Herder-Strasse 3, D-79104 Freiburg, Germany*
[2]*Institut für Physikalische Chemie, Universität Freiburg, Albertstrasse 23a, D-79104 Freiburg, Germany*
(Received 14 February 2003; published 6 June 2003)

We consider the dynamics of Vicsek fractals of arbitrary connectivity, models for hyperbranched polymers. Their basic dynamical properties depend on their eigenvalue spectra, which can be determined iteratively. This paves the way for theoretical studies to very high precision for regular, finite, arbitrarily large hyperbranched structures.

DOI: 10.1103/PhysRevE.67.061103 PACS number(s): 05.40.−a, 61.43.Hv, 83.80.Rs, 46.65.+g

The past years have seen a considerable increase in the investigations of hyperbranched macromolecular structures [1–8], objects which are topologically speaking trees (i.e., have no loops). Paradigmatic for the broad interest are the dendrimers [2–8], which are regular subsets of the Cayley tree: From a core sprout $f-1$ branches, which in the next generation have at their ends $f-1$ new branches each, f being the coordination number (number of nearest neighbors). Due to the exponential increase of the number of branches at each generation, the chemical synthesis usually stops after five or six generations. Furthermore, while the geometrical and dynamical properties of dendrimers have been studied in much detail, the objects are in many ways atypical for polymers; dendrimers are by far too regular and do not obey scaling [2–8]. Of much keener interest are general treelike structures (the so-called hyperbranched polymers). These are commonly synthesized in batch reactions and are, in principle, not limited in their growth [9–11].

Theoretically, in search of scaling [12,13], it is of importance to study other classes of regular hyperbranched polymers. One such class is given by the so-called Vicsek fractals [14–19], which are constructed iteratively. The generalized topology on which we focus is displayed in Fig. 1, which shows schematically in two-dimensions the $f=3$ structure. One starts from the object of generation $g=1$, consisting here of $f+1=4$ beads (open circles) arranged in starwise pattern, the central bead having three neighbors. To this object one attaches at the next generation, through f bonds, in starwise fashion, f identical copies of itself. Hence the next stage object ($g=2$) consists of 16 beads. The iteration is now obvious; Fig. 1 presents the finite $f=3$ Vicsek fractal for $g=3$. Note that in this way the regular pattern of Fig. 1 has a fractal dimension $\overline{d}_r$ of

$$\overline{d}_r=\frac{\ln(f+1)}{\ln 3}, \tag{1}$$

since increasing from the center the distance (radius) by a factor of 3 increases the number of beads inside it by $f+1$. Note that through Eq. (1), the extreme overcrowding found for dendrimers (where $\overline{d}_r=\infty$) does not appear in Vicsek fractals.

Many dynamical properties of connected structures [20] (such as the vibrational spectra, the relaxation modes, but also random walks over them) depend on the spectrum of the eigenvalues of their connectivity matrix $\mathbf{A}=(A_{ij})$. The off-diagonal elements A_{ij} are -1 if beads i and j are connected by a bond, and 0, otherwise; furthermore, the A_{ii} obey $A_{ii}=-\Sigma_{j\neq i}A_{ij}$.

Previous work has centered for finite Vicsek fractals on the case $f=4$; in this case Jayanthi and Wu [16–18] succeeded in determining the eigenvalues of $\mathbf{A}$ by computing the zeros of iteratively determined polynomials. Here we reanalyze the problem for general f and will show that the eigenvalues of Vicsek fractals can be obtained very easily, for arbitrary f and g, through an algebraic iterative procedure, which involves the Cardano solution for cubic equations [21]. These findings open the way to theoretically study the dynamics of arbitrarily large, finite Vicsek fractals.

We continue by displaying the procedure of the determination of the eigenvalues and present the recurrence formula, which allows us to obtain the eigenvalues of the $g+1$ generation from that of the g generation. From these quantities, we determine for the corresponding hyperbranched polymers both the average displacement of a monomer under a constant force as a function of time and also the mechanical storage modulus. As we will show, these quantities scale with exponents that depend only on the spectral dimension $\tilde{d}$ of the corresponding Vicsek fractal.

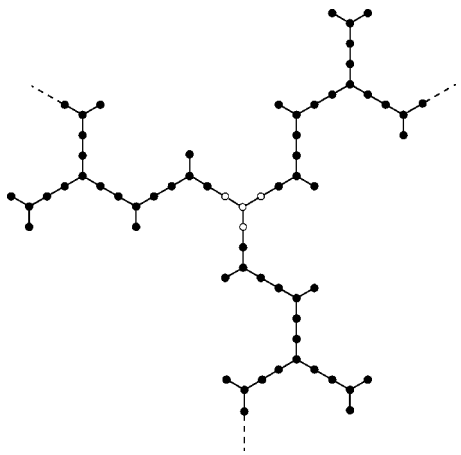

FIG. 1. Vicsek fractal at the stage $N=4^3$. Displayed is a regular pattern; note that the beads of a hyperbranched polymer in solution are very mobile.

The determination of the eigenvalues, i.e., the solution of $(\mathbf{A}-\lambda\mathbf{I})\mathbf{\Phi}=\mathbf{0}$ starts from realizing that the architecture of a Vicsek fractal displays f-coordinated centers (fCCs), connecting bonds, and also dangling bonds; hence each of its beads has either f, 2, or 1 neighbors. Setting ϕ_0 for the component of the fCC in $(\mathbf{A}-\lambda\mathbf{I})\mathbf{\Phi}=\mathbf{0}$, typical equations for its neighboring sites are

$$(f-\lambda)\phi_0=\sum_{j=1}^{f}\phi_j, \tag{2}$$

$$(2-\lambda)\phi_f=\phi_0+\phi_m, \tag{3}$$

$$(1-\lambda)\phi_1=\phi_0. \tag{4}$$

We now transform all such equations to a set involving the coordinates of nearest-neighboring fCCs only; by this we eliminate from these linear equations the variables of the intermediate and dangling beads. As can be verified by a short calculation, one obtains

$$[f-P(\lambda)]\tilde{\phi}_0=\sum_{j=1}^{f}\tilde{\phi}_j, \tag{5}$$

$$[2-P(\lambda)]\tilde{\phi}_f=\tilde{\phi}_0+\tilde{\phi}_m, \tag{6}$$

$$[1-P(\lambda)]\tilde{\phi}_1=\tilde{\phi}_0, \tag{7}$$

with

$$P(\lambda)=\lambda(\lambda-3)(\lambda-f-1). \tag{8}$$

This procedure, which is closely related to real-space decimation [22,23], can now be iterated k times, by which $P(\lambda)$ gets replaced by $p_k(\lambda)=P(p_{k-1}(\lambda))$.

For finite Vicsek fractals, Eq. (8) allows to determine the eigenvalues at generation $g+1$ from those at generation g through the relation

$$P(\lambda_i^{(g+1)})=\lambda_i^{(g)}. \tag{9}$$

Evidently, in this way, each previous eigenvalue gives rise to three new ones, a fact already noted in Refs. [15–19] for the case $f=4$. Moreover, at every generation one has the nondegenerate mode $\lambda_1=0$; furthermore, we find one nondegenerate mode corresponding to the eigenvalue $f+1$ and Δ_g new degenerate modes corresponding to the eigenvalue 1, where

$$\Delta_g=(f-2)(f+1)^{g-1}+1, \tag{10}$$

an expression that extends the findings of Refs. [15–18] to arbitrary f. From Eq. (10), one can readily compute the total number of nondegenerate, $N_g^{(nd)}$, and of degenerate, $N_g^{(d)}$, eigenvalues, obtaining $N_g^{(nd)}=1+(3^g-1)/2$ and $N_g^{(d)}=(3^g-1)/2+(f+1)^g-3^g$; hence $N_g^{(nd)}+N_g^{(d)}=(f+1)^g=N$, as it should be.

Furthermore, Eqs. (5), (8), and (9) can be used to compute the $\lambda_i^{(g)}$ iteratively, based on the roots of the polynomial

$$x^3-(f+4)x^2+3(f+1)x-a=0. \tag{11}$$

Introducing

$$p=\tfrac{1}{3}[f(f-1)+7], \tag{12}$$

$$q=\tfrac{1}{27}(5-f)(f+4)(2f-1), \tag{13}$$

and

$$\rho=|p/3|^{3/2}, \tag{14}$$

the roots of this polynominal are given by the Cardano solution, see Ref. [21]

$$x_\nu=(f+4)/3+2\rho^{1/3}\cos[(\phi+2\pi\nu)/3] \quad \text{with} \quad \nu \ \epsilon\{1,2,3\}, \tag{15}$$

where

$$\phi=\arccos[(a-q)/2\rho]. \tag{16}$$

Considering as in Ref. [24] the limit $a\to 0$ of Eq. (11), one obtains as spectral dimension,

$$\tilde{d}=\frac{2\ln(f+1)}{\ln(3f+3)}. \tag{17}$$

We used the above procedure, Eqs. (15) and (16), and determined exemplarily, for $f=2$, 3, 4, and 5, the eigenvalues of Vicsek fractals, recovering, for $f=4$, the former findings [15–19]. Here, for instance, for $f=3$ we readily obtain the eigenvalues for fractals up to $N=4^{13}$. For small structures it is also possible to fully diagonalize the corresponding **A** matrix and to verify the correctness of the procedure (eigenvalues and degeneracies). For larger systems, say up to $N=4^8$, we have used the fact that the **A** matrices are sparse, and computed their eigenvalues based on a modified Lanczos algorithm [25–27]. The agreement is perfect. Note, however, that in its standard form, the Lanczos procedure then supplies only the eigenvalues, but not their degeneracy. For even larger systems one reaches quite soon the limits of today's feasible numerical diagonalizations, while our iterative procedure is only limited by the number of digits employed.

We now consider the spectra which we obtained iteratively and display in Fig. 2 as a histogram, for the Vicsek fractal $N=4^{13}$, the density of states. Particularly striking are the discrete form of the spectrum, the multitude of forbidden bands, and the inherent symmetries. The eigenvalues belong, as also found for dual Sierpinski gaskets [28,29] and paralleling earlier results [17–19,22,23], to two sets: First, the localized modes, for which at a certain k one has $p_k(\lambda)=1$, and hence, as in Eq. (7), all fCCs of generation k and higher are immobile. Second, the modes with $p_k(\lambda)\neq 1$ for all k; these get infinitely iterated according to Eqs. (12)–(16), creating thus a Cantor set. Furthermore, as we will show, this spectrum gives rise to rather smooth relaxation forms, which scale according to relations based on the spectral dimension.

We now turn to regular hyperbranched structures, which we model as generalized Gaussian structures (GGSs) [30], the extension of the classical Rouse model [31–33] to net-

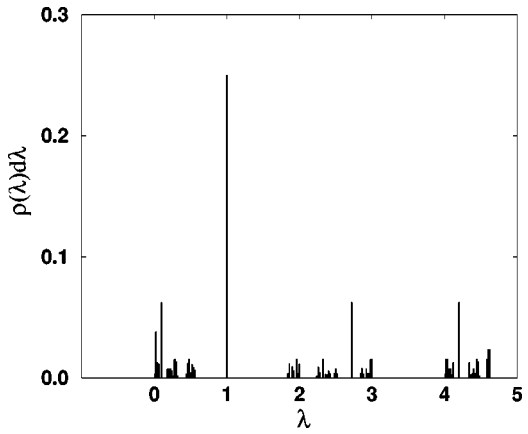

FIG. 2. Histogram of the density of states $\rho(\lambda)d\lambda$ of a Vicsek fractal at the stage $N=4^{13}$ in bins of width $\Delta=0.02$.

works. A GGS consists of N beads subject to friction (with friction constant ζ) connected to each other by springs (with elasticity constant K). In the Langevin formalism, the position vector $\mathbf{r}_l(t)$ of the lth bead of the GGS, subject to the external force $\mathbf{F}_l(t)$, obeys [6,7]

$$\zeta\frac{d\mathbf{r}_l(t)}{dt}+K\sum_{m=1}^{N}A_{lm}\mathbf{r}_m(t)=\mathbf{F}_l(t)+\zeta\mathbf{w}_l(t), \qquad (18)$$

where $\mathbf{A}$ is (as before) the connectivity matrix of the GGS, and $\zeta\mathbf{w}_l(t)$ is the thermal noise (here assumed to be Gaussian, with zero mean value).

We focus on the motion (drift and stretching) of the GGS under a constant external force $\mathbf{F}(t)=F\theta(t)\mathbf{e}_y$, switched on at $t=0$ and acting on a single bead in the y direction. The displacement along the y direction, $Y(t)$, which then follows, reads the following after averaging both over the fluctuating forces $\mathbf{w}_l(t)$ and over all the beads of the GGS [6,7,34]:

$$\overline{Y(t)}=\frac{F}{\zeta N}t+\frac{F\tau_0}{\zeta}\frac{1}{N}\sum_{i=2}^{N}\frac{1-\exp[-\lambda_i(t/\tau_0)]}{\lambda_i}, \qquad (19)$$

with $\tau_0=\zeta/K$ and $\lambda_1=0$. Equation (19) is very simple; it involves *only* the eigenvalues λ_i (but not the eigenvectors) of the connectivity matrix $\mathbf{A}$. One may note that in Eq. (19), due to $\lambda_1=0$, the motion of the center of mass has separated automatically from the rest. Clearly, the behavior of the motion for extremely short and for very long times is obvious: One has in the limit of very short times, from Eq. (19), $\overline{Y(t)}\sim Ft/\zeta$, whereas for very long times one attains $\overline{Y(t)}\sim Ft/(N\zeta)$. These are very general features, which make clear that the particular structure of the GGS under investigation (and thus information about its structural matrix $\mathbf{A}$) is revealed only in the intermediate time domain.

Apart from $\overline{Y(t)}$, a quantity which nowadays may be accessed through micromechanical manipulations [35], classical experiments focus on the mechanical and dielectric relaxation. Most mechanical experiments probe the complex dynamic modulus $G^*(\omega)$, i.e., its real $G'(\omega)$ and imaginary

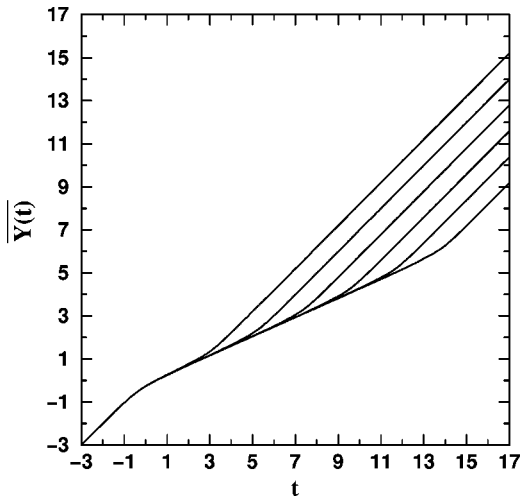

FIG. 3. The averaged monomer displacement $\overline{Y(t)}$ under the action of an external force. Displayed are, in double-logarithmic scales to basis 10 and in dimensionless units, both t and the normalized $\overline{Y(t)}$ for $N=4^3$, 4^5, 4^7, 4^9, 4^{11}, and 4^{13} from above.

$G''(\omega)$ components, (the storage and the loss moduli [36,37]). For instance, $G'(\omega)$ is given by, see Eqs. (4.159) of Ref. [32],

$$G'(\omega)=C\sum_{i=2}^{N}\frac{(\omega\tau_0/2\lambda_i)^2}{1+(\omega\tau_0/2\lambda_i)^2}, \qquad (20)$$

where C is, for our purposes here, a constant.

For Vicsek fractals, we can now use the recursively obtained eigenvalues in order to calculate the relaxation quantities, Eqs. (19) and (20). We start by focusing on the averaged displacement $\overline{Y(t)}$, Eq. (19), in which we set $\tau_0=1$ and $F/\zeta=1$. The results are presented in Fig. 3 for finite Vicsek fractals, ranging from $N=4^3$ to $N=4^{13}$. Note that in Fig. 3 the scales are doubly logarithmic. Clearly evident from the figure is that at long times one reaches the domain $\overline{Y(t)}\sim Ft/(N\zeta)$ and that at short times one has $\overline{Y(t)}\sim Ft/\zeta$. Because of the N dependence of $\overline{Y(t)}$, in Fig. 3 curves belong-

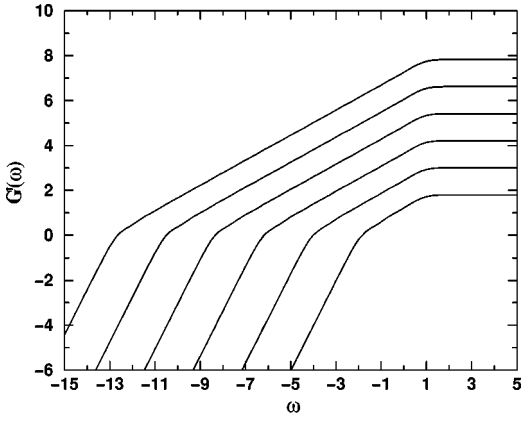

FIG. 4. The normalized storage modulus $G'(\omega)$, displayed in dimensionless units and double-logarithmic scales to basis 10 for $N=4^3$, 4^5, 4^7, 4^9, 4^{11}, and 4^{13} from below.

ing to fractals of different sizes are shifted with respect to each other. Now, typical for the *fractal* structure is the domain at intermediate times, in which the different curves merge. In the double-logarithmic scales of Fig. 3 this subdiffusive scaling domain appears (as in Fig. 1(a) of Ref. [34]) as a straight line; as we proceed to show its slope tends to $\gamma = 1 - \tilde{d}/2$.

We can use now the slopes of the curves in Fig. 3 to determine numerically the slope γ. In fact we find for the largest fractal considered, namely, $N = 4^{13}$, the best linear fit in the region between $t = 10^4$ and 10^9. In this region a linear approximation leads to $\gamma = 0.442$, to be compared with $1 - \tilde{d}/2 = 0.44211\ldots$. The accuracy attained indeed allows to assess [38] that the sole fractal parameter of importance is $\tilde{d}$. As shown by us previously, analogous findings hold for Sierpinski-type structures [28,29,39].

We turn now to the storage modulus $G'(\omega)$, given by Eq. (20) and presented in Fig. 4. Here again we used finite fractals extending from $N = 4^3$ to $N = 4^{13}$; we plot Eq. (20) in dimensionless units, by setting $\tau_0 = 1$ and $C = 1$. Clearly evident from Fig. 4 are the limiting, connectivity-independent behaviors at very small and very high ω; for $\omega \ll 1$ one has $G'(\omega) \sim \omega^2$ and for $\omega \gg 1$ one finds $G'(\omega) \sim \omega^0$. Again the fractal connectivity aspect is given by the in-between region; here by going from $N = 4^3$ to $N = 4^{13}$ we have a change in the minimal slope from 0.621 to 0.557. The last value should be compared to $\tilde{d}/2 = 0.557\,88\ldots$. Also, one may note from Figs. 3 and 4 that if N is 64, due to the substantial crossover domains, the slopes which are inferred are rather far from $1 - \tilde{d}/2$ and from $\tilde{d}/2$, respectively; to obtain these values accurately, large GGS are needed.

A point which deserves attention is that the curves depicted in Figs. 3 and 4 are very smooth, and that they do not betray the very complex structure of the Cantor set which underlies them.

We acknowledge gratefully the help of the Deutsche Forschungsgemeinschaft. A.B. thanks the Fonds der Chemischen Industrie and BMBF for their support.

[1] J. Roovers, in *Star and Hyperbranched Polymers*, edited by M. K. Mishra and S. Kobayashi (Marcel Dekker, New York, 1999), p. 285.
[2] R. La Ferla, J. Chem. Phys. **106**, 688 (1997).
[3] C. Cai and Z.Y. Chen, Macromolecules **30**, 5104 (1997).
[4] Z.Y. Chen and C. Cai, Macromolecules **32**, 5423 (1999).
[5] F. Ganazzoli, R. La Ferla, and G. Raffaini, Macromolecules **34**, 4222 (2001).
[6] P. Biswas, R. Kant, and A. Blumen, Macromol. Theory Simul. **9**, 56 (2000).
[7] P. Biswas, R. Kant, and A. Blumen, J. Chem. Phys. **114**, 2430 (2001).
[8] A.A. Gurtovenko, Yu.Ya. Gotlib, and A. Blumen, Macromolecules **35**, 7481 (2002).
[9] A. Sunder, R. Hanselmann, H. Frey, and R. Mülhaupt, Macromolecules **32**, 4240 (1999).
[10] A. Sunder, J. Heinemann, and H. Frey, Chem.-Eur. J. **6**, 2499 (2000).
[11] C. von Ferber and A. Blumen, J. Chem. Phys. **116**, 8616 (2002).
[12] H. Schiessel, Ch. Friedrich, and A. Blumen, in *Applications of Fractional Calculus in Physics*, edited by R. Hilfer (World Scientific, Singapore, 2000), p. 331.
[13] I.M. Sokolov, J. Klafter, and A. Blumen, Phys. Today **55**(11), 48 (2002).
[14] T. Vicsek, *Fractal Growth Phenomena* (World Scientific, Singapore, 1989).
[15] C.S. Jayanthi, S.Y. Wu, and J. Cocks, Phys. Rev. Lett. **69**, 1955 (1992).
[16] C.S. Jayanthi and S.Y. Wu, Phys. Rev. B **48**, 10 188 (1993).
[17] C.S. Jayanthi and S.Y. Wu, Phys. Rev. B **48**, 10 199 (1993).
[18] C.S. Jayanthi and S.Y. Wu, Phys. Rev. B **50**, 897 (1994).
[19] W.A. Schwalm, M.K. Schwalm, and M. Giona, Phys. Rev. E **55**, 6741 (1997).
[20] *Fractals and Disordered Systems*, edited by A. Bunde and S. Havlin (Springer-Verlag, Berlin, 1996).
[21] I.N. Bronstein and K.A. Semendjajev, *Taschenbuch der Mathematik* (Nauka, Moscow; Teubner, Leipzig, 1985), Chap. 2.4.2.
[22] E. Domany, S. Alexander, D. Bensimon, and L.P. Kadanoff, Phys. Rev. B **28**, 3110 (1983).
[23] R. Rammal, J. Phys. (France) **45**, 191 (1984).
[24] S.H. Liu, Phys. Rev. B **30**, 4045 (1984).
[25] C. Lanczos, J. Res. Natl. Bur. Stand., Sect. B **45**, 225 (1950).
[26] J.K. Cullum and R. Willoughby, *Lanczos Algorithms for Large Symmetric Eigenvalue Problems* (Birkhäuser, Boston, 1985), Vols. I and II.
[27] Th. Koslowski and W. von Niessen, J. Comput. Chem. **14**, 769 (1993).
[28] A. Blumen and A. Jurjiu, J. Chem. Phys. **116**, 2636 (2002).
[29] A. Jurjiu, Ch. Friedrich, and A. Blumen, Chem. Phys. **284**, 221 (2002).
[30] J.-U. Sommer and A. Blumen, J. Phys. A **28**, 6669 (1995).
[31] P.E. Rouse, J. Chem. Phys. **21**, 1272 (1953).
[32] M. Doi and S.F. Edwards, *The Theory of Polymer Dynamics* (Clarendon Press, Oxford, 1986).
[33] A.Yu. Grosberg and A.R. Khokhlov, *Statistical Physics of Macromolecules* (AIP Press, New York, 1994).
[34] H. Schiessel, Phys. Rev. E **57**, R5775 (1998).
[35] R. Granek and J. Klafter, Europhys. Lett. **56**, 15 (2001).
[36] I.M. Ward, *Mechanical Properties of Solid Polymers*, 2nd ed. (Wiley, Chichester, 1985).
[37] J.D. Ferry, *Viscoelastic Properties of Polymers*, 3rd ed. (Wiley, New York, 1980).
[38] M.E. Cates, J. Phys. (France) **46**, 1059 (1985).
[39] A. Jurjiu, Th. Koslowski, and A. Blumen, J. Chem. Phys. **118**, 2398 (2003).